

Temperatures of fragment kinetic energy spectra

Wolfgang Bauer

*Institute for Nuclear Theory, University of Washington, Seattle, Washington 98195
and National Superconducting Cyclotron Laboratory and Department of Physics and Astronomy,
Michigan State University, East Lansing, Michigan 48824*

(Received 6 October 1994)

Multifragmentation reactions without large compression in the initial state (proton-induced reactions, reverse kinematics, projectile fragmentation) are examined, and it is verified quantitatively that the high temperatures obtained from fragment kinetic energy spectra and lower temperatures obtained from observables such as level population or isotope ratios can be understood in a common framework.

PACS number(s): 25.70.Pq

The phenomenon of nuclear multifragmentation, the decay of highly excited nuclear matter into (nucleons and) several fragments of size $A_f > 5$, has been observed in proton-induced and heavy ion reactions [1, 2]. Very recently, similar multifragmentation events have also been observed in the disintegration of C_{60} -fullerenes ("buckyballs") after bombardment with high-energy heavy ions [3]. It is clear by now that there is probably no one single mechanism responsible for the multitude of different fragmentation scenarios which range from sequential binary emission processes at low excitation energies [4] over statistical multifragmentation [5] to explosive vaporization. The most exciting possibility is probably the occurrence of a second-order phase transition at the critical point of nuclear matter [6–8].

The majority of theoretical investigations has been aimed at understanding the fragment mass distributions. However, there is considerable interest in fragment kinetic energy spectra, and the present paper is also concerned with this topic. In high-energy proton-induced [6] and relativistic projectile fragmentation [9] reactions one observes Boltzmann-like kinetic energy spectra of intermediate mass fragments with temperatures, for which the fragment mass dependence has been parametrized [6] as $T_f = T_0 (A_r - A_f)/A_r$, where A_r is the mass of the recoil residue. The temperature T_0 typically has a value ≈ 15 MeV, much larger than nuclear temperatures extracted from isotope ratios or level population ratios [10], and also much larger than typical temperatures (≈ 5 –8 MeV) used in statistical models [5] to reproduce the experimental mass yield curves.

Here it is argued that the comparatively high value of T_f is a consequence of the addition of the Fermi momenta of the individual nucleons in the fragment and thus a consequence of the Fermi-Dirac nature of nucleons. The single-particle model is employed. It previously was successfully used [11–13] to explain the observed dispersion in fragment transverse momentum spectra generated in projectile fragmentation.

One starts with an ensemble of A nucleons at (internal) temperature T_{in} . In the single-particle picture their momentum distribution (in the nonrelativistic limit) is given by

$$\rho(\mathbf{p}) = (1 + \exp[(p^2/2m - \mu)/T_{in}])^{-1}, \quad (1)$$

where μ is the chemical potential. Adding up the individual momentum vectors of all A_f nucleons in a fragment one then arrives at the momentum distribution of the fragment

$$\rho(\mathbf{P}_f) = \int \prod_{i=1}^{A_f} \{d^3 p_i \rho(\mathbf{p}_i)\} \delta^3\left(\mathbf{P}_f - \sum_{i=1}^{A_f} \mathbf{p}_i\right). \quad (2)$$

This addition procedure is of course nothing else but a random walk in momentum space and thus in the class of problems first posed by Pearson [14]. Since the single-particle probability distribution has 0 average and a fixed variance σ^2 , the central limit theorem of Gauss applies in the present case, and — for a sufficiently large number of steps, A_f , in the random walk — the probability distribution can be written as

$$\rho(\mathbf{P}_f) = \frac{1}{\sqrt{2\pi A_f \sigma^2}} \exp\left(-\frac{P_f^2}{2A_f \sigma^2}\right). \quad (3)$$

Using the nonrelativistic approximation $E_f = P_f^2/(2m_N A_f)$, we therefore find an exponentially falling kinetic energy spectrum for the fragments

$$\rho(E_f) = \frac{2}{\sqrt{\pi T_f^3}} \sqrt{E_f} \exp\left(-\frac{E_f}{T_f}\right), \quad (4)$$

where in this picture the apparent temperature T_f is given by

$$T_f = \sigma^2/m_N. \quad (5)$$

What exactly constitutes a sufficiently large number of steps is not *a priori* clear. However, in Fig. 1, I answer this question numerically by solving Eq. (2) with a dispersion of $\sigma^2 = \frac{2}{5} E_F m_N = 0.014 \text{ GeV}^2$. (This choice will become more apparent below.) For each fragment mass 5×10^6 events were generated. Displayed are the resulting distributions (histograms) for $A_f = 2, 3, 5, 12, 100$. One can clearly see that even a very small number of steps (between 5 and 12) are sufficient to approach the limit given by Gauss, Eq. (4) (solid line).

In the simple Fermi-gas model at 0 temperature, the variance in the momentum distribution is given by $\sigma^2 = p_F^2/5$, where p_F is the Fermi momentum. However, as pointed out by Goldhaber [12], there is the additional constraint that the momenta of all A nucleons combined add up to 0. This leads to

$$\sigma^2 = \frac{A - A_f}{A - 1} \langle p_i^2 \rangle. \quad (6)$$

The term $(A - A_f)/(A - 1)$ is the recoil correction due to total momentum conservation. It explains the experimentally observed dependence of T_f on A_f [6].

Inserting Eq. (6) into Eq. (5) leads to an apparent fragment kinetic temperature

$$T_f = \frac{1}{m_N} \frac{A - A_f}{A - 1} \langle p_i^2 \rangle = \frac{A - A_f}{A - 1} \frac{2}{3} \langle E_k \rangle, \quad (7)$$

where $\langle E_k \rangle$ is the average kinetic energy per nucleon as obtained from the single particle model. In the finite temperature case considered here this average is

$$\langle E_k \rangle = \int_0^\infty d\epsilon \frac{\epsilon^{3/2}}{1 + \exp[(\epsilon - \mu)/T_{in}]} \Big/ \int_0^\infty d\epsilon \frac{\epsilon^{1/2}}{1 + \exp[(\epsilon - \mu)/T_{in}]} \quad (8)$$

In the limit $T_{in} \rightarrow 0$, we obtain $\mu \rightarrow E_F$ and $\{1 + \exp[(\epsilon - \mu)/T_{in}]\}^{-1} \rightarrow \theta(E_F - \epsilon)$, and the average of Eq. (8) becomes simply $\langle E_k(T_{in}=0) \rangle = \frac{3}{5} E_F$, and consequently, the apparent fragment kinetic temperature at $T_{in}=0$ will *not* be 0, but rather

$$T_f(T_{in}=0) = \frac{A - A_f}{A - 1} \frac{2}{5} E_F. \quad (9)$$

In the case $T_{in} > 0$, the single particle model is still applicable. Its assumptions are not dependent on any sudden approximation (as frequently applied in the study of projectile fragmentation), but they also hold for a system in equilibrium at some finite temperature. This was already pointed out by Goldhaber [12]. In this case, the numerical solution of Eq. (8) inserted into Eq. (7) will yield the desired answer, the dependence of the apparent temperature as extracted from fragment kinetic energy spectra on the "real" temperature of the system. For small temperatures T_{in} one can perform a Sommerfeld expansion of these equations around $T_{in} = 0$. This yields the approximation

$$\mu \approx E_F \left(1 - \frac{\pi^2}{12} \left(\frac{T_{in}}{E_F} \right)^2 + \mathcal{O} \left(\frac{T_{in}}{E_F} \right)^4 \right) \quad (10)$$

for the chemical potential and for the apparent fragment temperature the useful expression

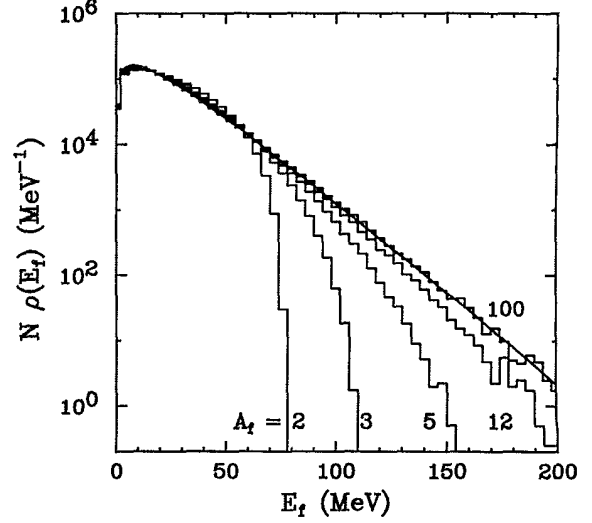


FIG. 1. Fragment kinetic energy spectra for different masses (histograms) from solving Eq. (2) with a value for the variance of 0.014 GeV^2 . The solid line is the Gauss limit, Eq. (4).

$$T_f(T_{in}) \approx \frac{A - A_f}{A - 1} \frac{2}{5} E_F \left(1 + \frac{5\pi^2}{12} \left(\frac{T_{in}}{E_F} \right)^2 + \mathcal{O} \left(\frac{T_{in}}{E_F} \right)^4 \right), \quad (11)$$

which works to better than five percent up to $T_{in}/E_F = 0.3$. Figure 2 shows a comparison of the numerical solution [ignoring the recoil correction term $(A - A_f)/(A - 1)$] (solid line) as well as the approximation of Eq. (11).

Bertsch [13] has pointed out that there is (for $T_{in} = 0$) a suppression of the dispersion due to Pauli correlations, which can amount to about 30% in the projectile fragmentation of ^{40}Ca . This effect is not included in the simple estimate provided here.

The effects of final state interaction, the emission of a nucleon from the excited pre-fragment, on the fragment kinetic energy distribution is also small [13]. Typical thermal momenta of single nucleons are $p_t \approx \sqrt{3 m_n T_{in}}$. This results in corrections of the order $(p_t/P_f)^2 \approx T_{in}/A_f T_f$, about 5% for fragments like carbon. The final state Coulomb interaction will mainly shift the energies upward, and with it raise the temperature T_f slightly.

The exact value of T_f as a function of T_{in} depends on E_F , which in turn depends on the freeze-out density as $E_F(\rho) = E_F(\rho = \rho_0) (\rho/\rho_0)^{2/3}$. It is, perhaps, instructive to insert some typical numbers: If we assume a

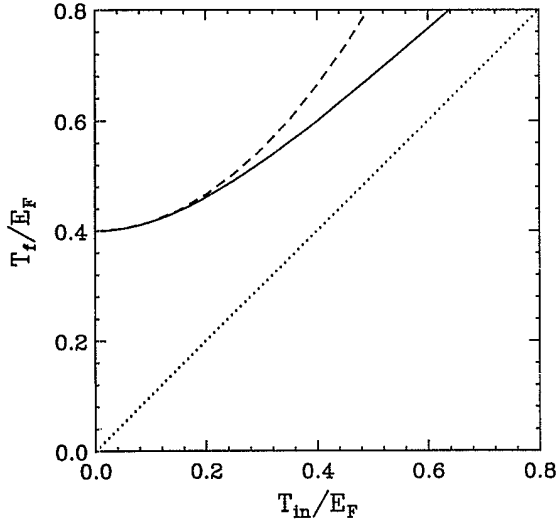


FIG. 2. Apparent temperature of fragment kinetic energy spectra (in units of the Fermi energy) as a function of the temperature, T_{in} of the Fermi gas. Solid line: numerical solution of Eq. (8) inserted into Eq. (7). Dashed line: analytic approximation, Eq. (11).

freeze-out density of $0.5 \rho_0$, and a temperature of $T_{in} = 6$ MeV, then we obtain a Fermi energy of 24 MeV, and a slope constant (ignoring the recoil correction) of $T_f = 12$ MeV. This number is of the order obtained by projectile

fragmentation reactions, and it therefore is possible that fragmentation reactions of this kind are not really a cold breakup of nuclei at nuclear matter density (as is conventionally assumed), but the fragmentation of a more dilute system at higher internal temperature.

In summary, by application of the single particle model it was shown that it is possible to understand the high values of apparent fragment kinetic energy spectra temperatures as compared to temperatures extracted from isotope ratios or level population ratios in proton-induced or reverse kinematics fragmentation reactions. One may speculate that this basic mechanism can also qualitatively explain similar observations for heavy ion induced fragmentation events with sizeable compression (by inclusion of radial flow momentum components), but the model employed here might be too simple for this case.

Many useful discussions with the participants of the workshop "Hot and Dense Nuclear Matter," in particular, J. Bondorf, G. Bertsch, J. Randrup, and W. Friedman, are acknowledged. This work was supported by the National Science Foundation under Grant No. PHY-9403666 and a Presidential Faculty Fellow award. In addition, I thank the Institute for Nuclear Theory at the University of Washington for its hospitality and the U.S. Department of Energy for partial support during the completion of this work.

- [1] J. Hüfner, Phys. Rep. **125**, 131 (1985).
- [2] L.G. Moretto and G.J. Wozniak, Annu. Rev. Nucl. Part. Sci. **43**, 379 (1993).
- [3] T. LeBrun *et al.*, Phys. Rev. Lett. **72**, 3965 (1994).
- [4] W.A. Friedman and W.G. Lynch, Phys. Rev. C **28**, 16 (1983).
- [5] J. Randrup and S.E. Koonin, Nucl. Phys. **A356**, 223 (1981); J.P. Bondorf, Nucl. Phys. **A387**, 25c (1982); D.H.E. Gross *et al.*, Z. Phys. A **309**, 41 (1982).
- [6] R.W. Minich *et al.*, Phys. Lett. **118B**, 458 (1982); A.S. Hirsch *et al.*, Phys. Rev. C **29**, 508 (1984).
- [7] W. Bauer *et al.*, Phys. Lett. **150B**, 53 (1985); W. Bauer *et al.*, Nucl. Phys. **A452**, 699 (1986); W. Bauer, Phys. Rev. C **38**, 1297 (1988).
- [8] X. Campi, J. Phys. A **19**, L917 (1986); X. Campi, Phys. Lett. B **208**, 351 (1988).
- [9] D.E. Greiner *et al.*, Phys. Rev. Lett. **42**, 152 (1975).
- [10] D.J. Morrissey *et al.*, Annu. Rev. Nucl. Part. Phys. **44**, 27 (1994).
- [11] H. Feshbach and K. Huang, Phys. Lett. **47B**, 300 (1973).
- [12] A.S. Goldhaber, Phys. Lett. **53B**, 306 (1974); A.S. Goldhaber, Phys. Rev. C **17**, 2243 (1978).
- [13] G.F. Bertsch, Phys. Rev. Lett. **46**, 472 (1981).
- [14] K. Pearson, Nature **72**, 294 (1905); see also Lord Rayleigh, *ibid.* **72**, 318 (1905).